Directional Properties of Wind-Generated Surface Waves
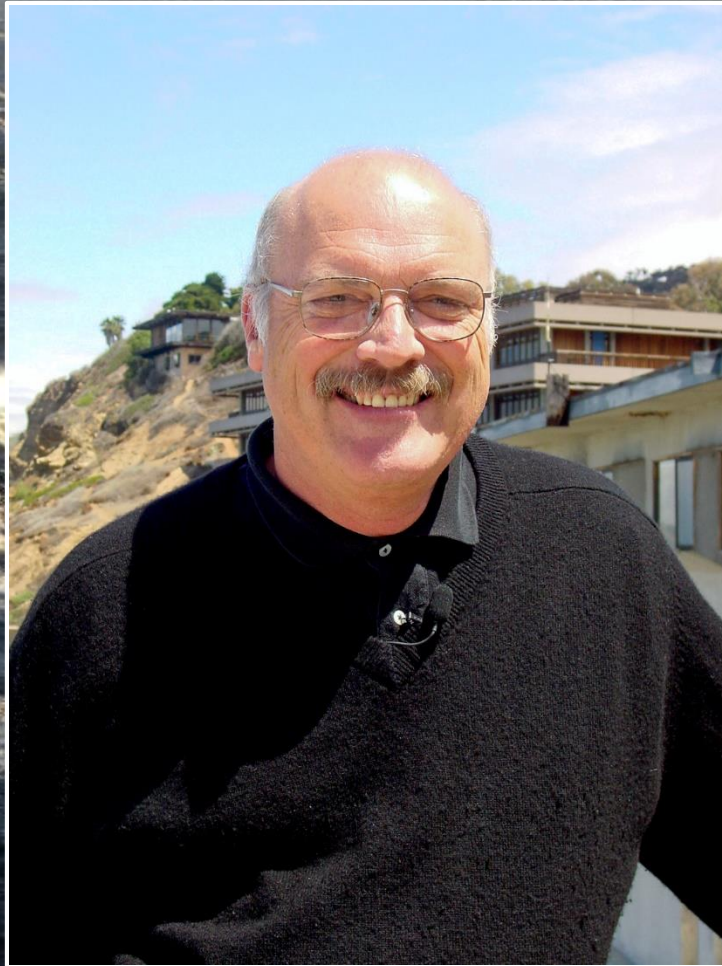
Luc Lenain, Ken Melville and Nick Statom

Scripps Institution of Oceanography, UCSD

November 13 2019

Ken Melville 1946-2019

Directional Properties of Wind-Generated Surface Waves

Luc Lenain, Ken Melville and Nick Statom
Scripps Institution of Oceanography, UCSD

November 13 2019

- To investigate the properties of directional wave field across the equilibrium-saturation ranges from airborne lidar

- To characterize the bimodal distribution found in the directional wave spectrum

- To parameterize the upper wavenumber limit of the equilibrium range, of significant importance to wave modelling

Lenain, L. and W.K. Melville, 2017: Measurements of the Directional Spectrum across the Equilibrium Saturation Ranges of Wind-Generated Surface Waves. J. Phys. Oceanogr., 47, 2123–2138, https://doi.org/10.1175/JPO-D-17-0017.1

Theoretical foundation of wave generation by wind established in the 1950s (Miles 1957, Phillips 1957) and non-linear wave-wave interaction in the 60s (Phillips 1960, Hasselmann 1962, Zakharov and Filonenko 1967).

Wind wave simulations are generally represented by the **Radiative transfer equation:**

$$\frac{dN(x,k,t)}{dt} = \frac{S}{\sigma} = \frac{S_{in} + S_{nl} + S_{ds}}{\sigma}$$

where $N(x,k,t) = \dfrac{F(x,k,t)}{\sigma}$ is the wave action spectral density, **x** the horizontal position,

k is the wavenumber, t is time, σ the intrinsic frequency.

Energy density "source terms"

S_{in} : wind input (Snyder 1981, Janssen 1992) (i.e. wave growth due to wind)
S_{nl} : non-linear wave-wave interactions (Webb-Resio-Tracy WRT method using Van Vledder's WaveWatch III implementation)
S_{ds} : dissipation, primarily due to wave breaking (Alves and Banner, 2003; Romero and Melville 2010, 2012)

SCRIPPS INSTITUTION OF OCEANOGRAPHY *UC San Diego*

Phillips (1985) considers the existence of an equilibrium range, where

$$\frac{dN(x,k,t)}{dt} = \frac{S}{\sigma} = \frac{S_{in} + S_{nl} + S_{ds}}{\sigma} = 0$$
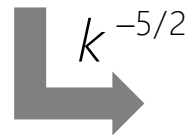
Assuming that the **non-linear energy flux**, **wind forcing** and **energy dissipation** (from breaking) are in **balance**, **proportional** and of **similar magnitude**
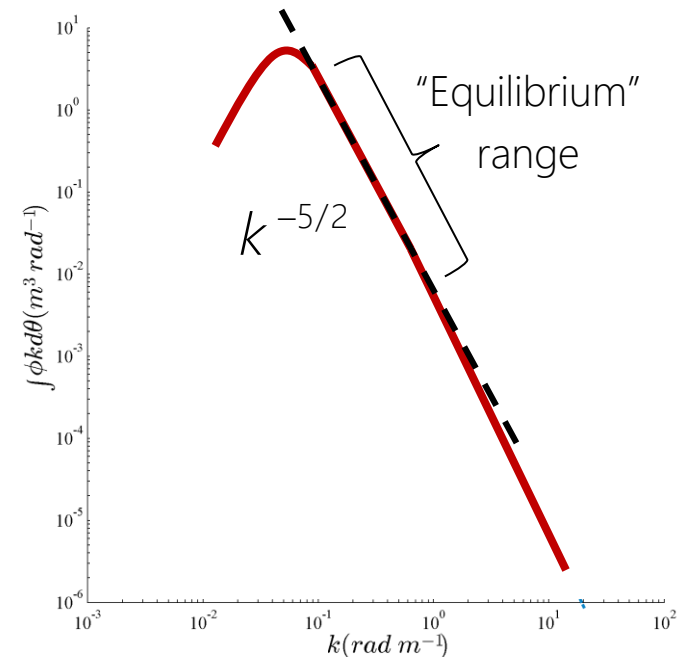
$$S_{in} \propto S_{nl} \propto S_{ds}$$

Leading to a directional wavenumber spectrum in the equilibrium range of the form

$$\phi(k,\theta) \propto (\cos\theta)^p u_* k^{-7/2}$$

where p ~ $\frac{1}{2}$

$k^{-5/2}$

Azimuthal integration to compute omnidirectional spectrum

$\emptyset(k,\theta)$ is the directional wavenumber spectrum in polar coordinate

Beyond the equilibrium range, we find the saturation range, where the **primary balance** is between **wind forcing** and **energy dissipation** (from breaking), as the **non-linear energy flux gets much smaller.**

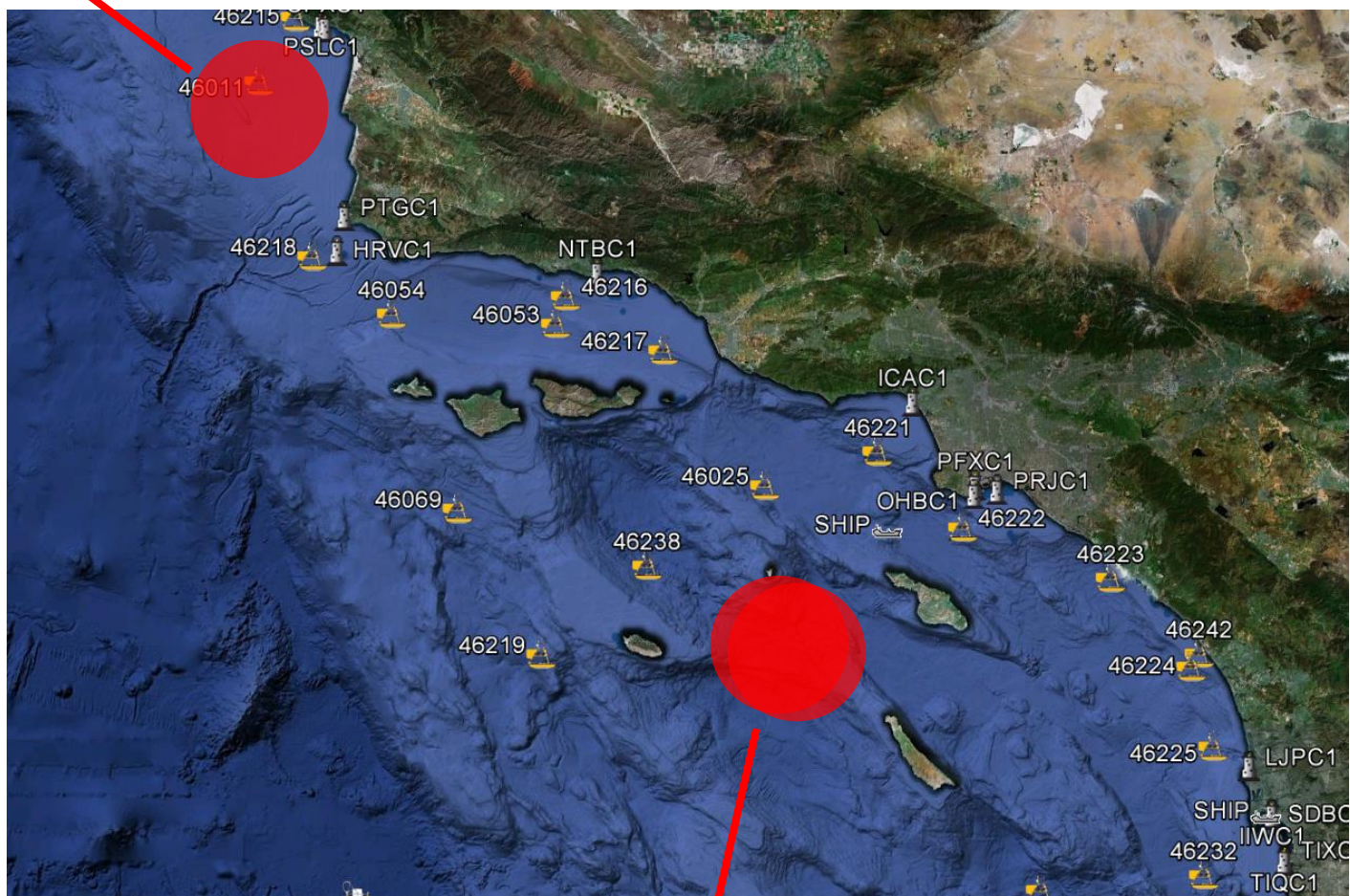Leading to a directional wavenumber spectrum for this range

$$\phi(k,\theta) \propto Bk^{-4}$$

k^{-3}

Azimuthal integration to compute omnidirectional spectrum

Observational evidences of the transition from equilibrium to saturation ranges are very limited, motivating this work.
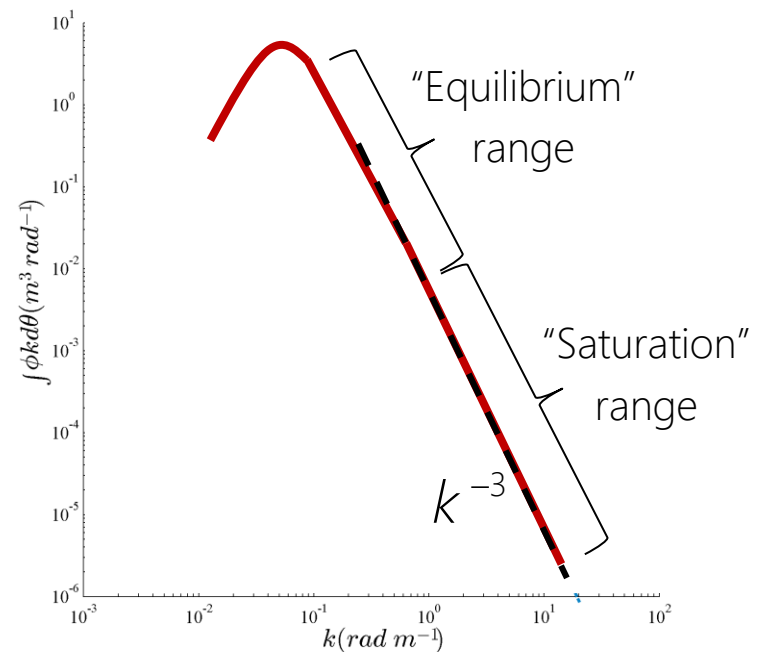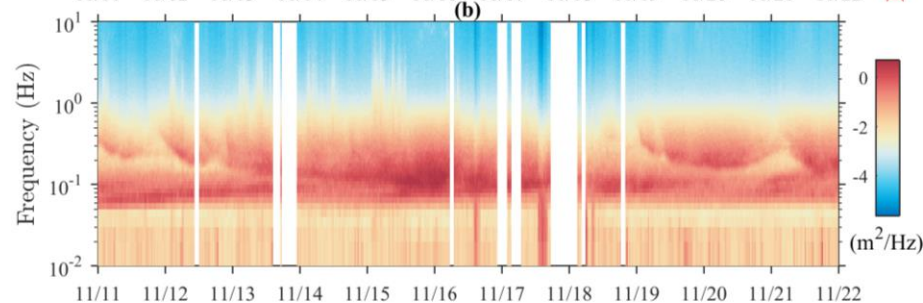
Innershelf DRI (2017)

SOCAL2013 & LCDRI2017

SOCAL2013 experiment – November 2013

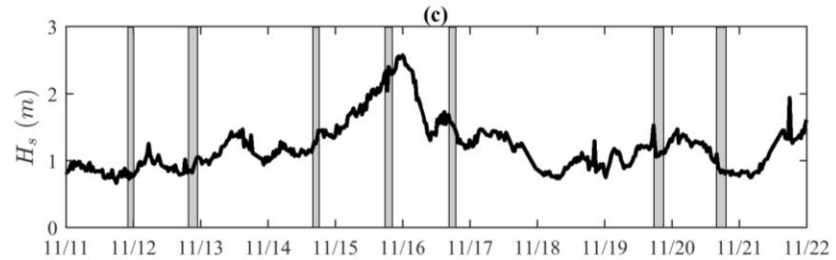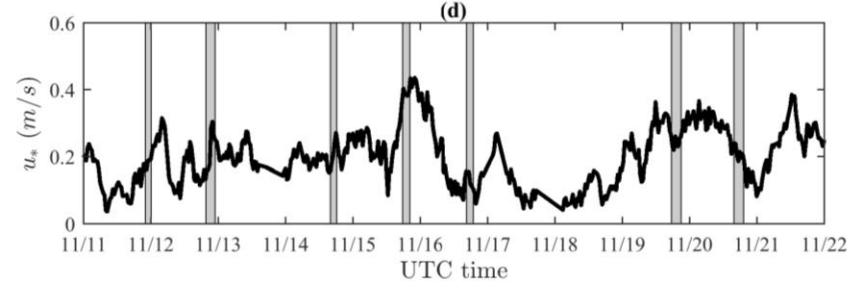Plan view

Photo credit: Evan Walsh
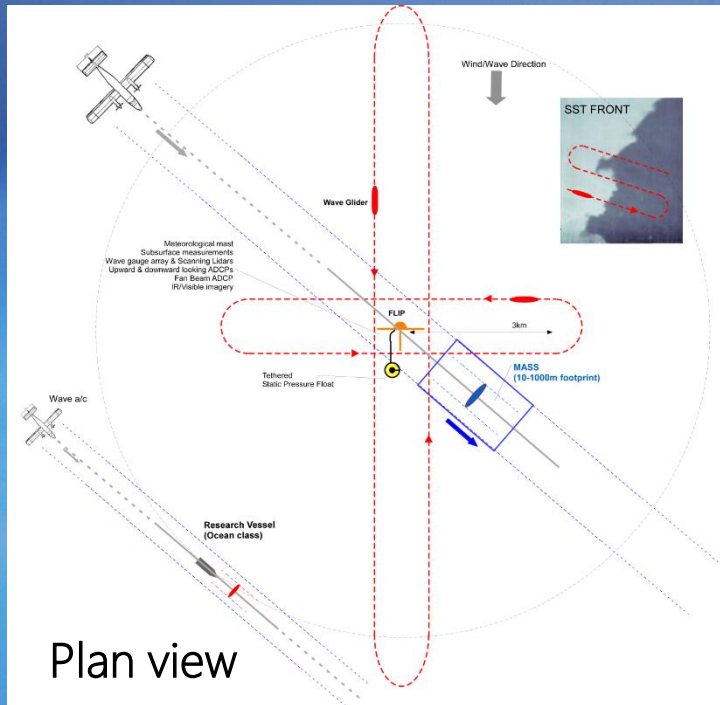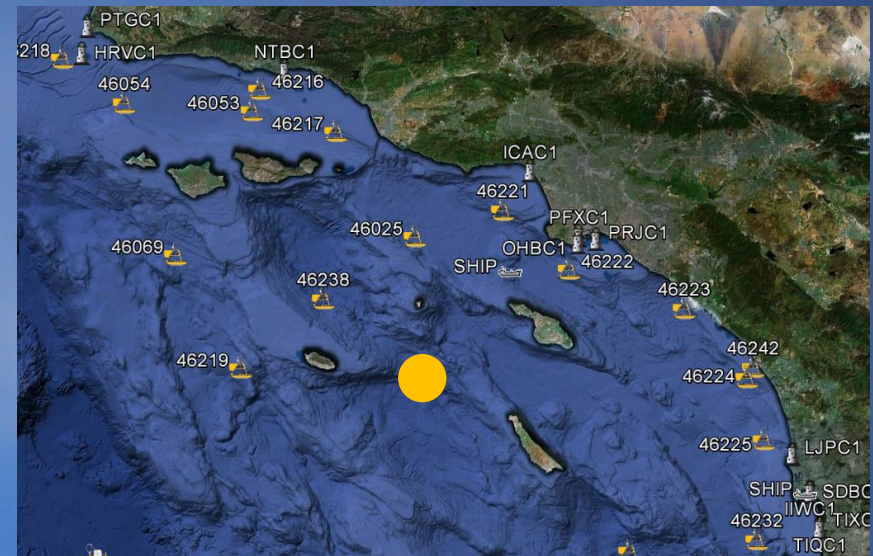
Wind
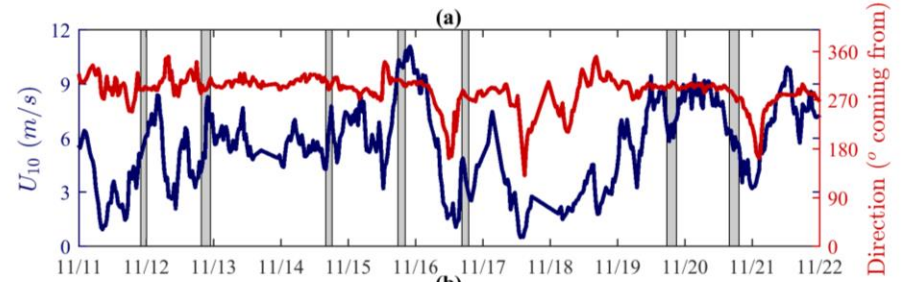
Wave frequency spectrogram

Significant wave height

Friction velocity
(atmospheric)

(Flight times in gray)

SIO Modular Aerial Sensing System (MASS)

NDBC Station 42040
29.212°N 88.207°W
19 Oct 2011

Spatial resolution
0.25x0.25m
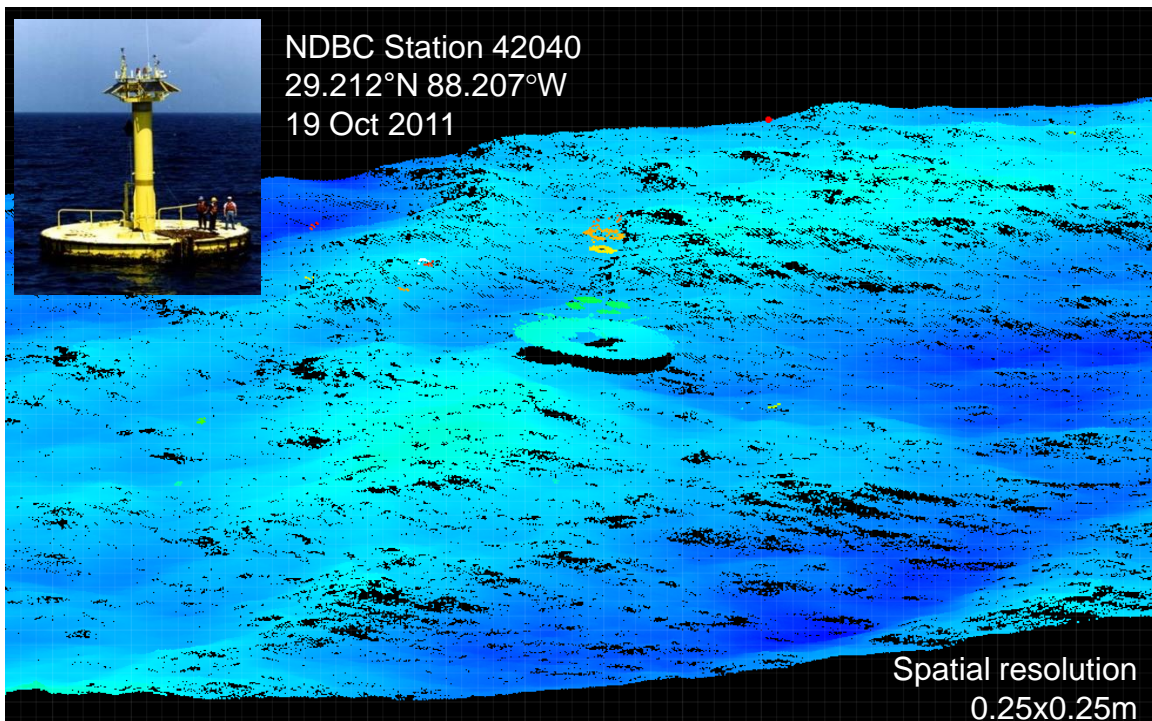
Example of surface elevation as measured from the MASS during a 2011 experiment in the Gulf of Mexico, flying above NDBC buoy #42040. (wind~12m/s, Hs = 3.1m)
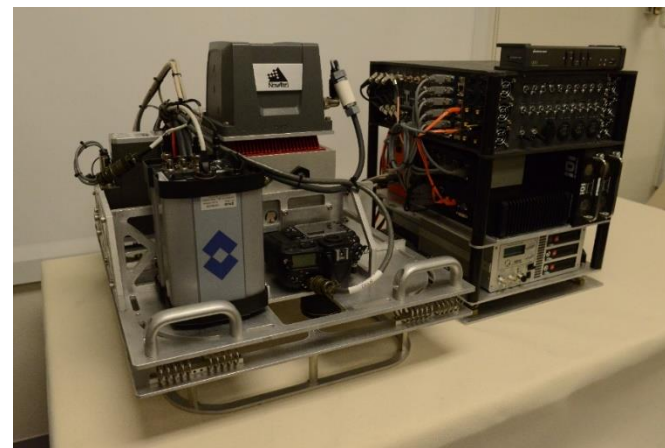

Instrumentation		Measurement
Scanning Waveform Lidar	Riegl Q680i	Surface wave, surface slope, directional wave spectra (vert. accuracy ~2-3cm)
Long-wave IR Camera	FLIR SC6000 (QWIP)	Ocean surface processes, wave kinematics and breaking, frontal processes
High-Resolution Video	JaiPulnix AB-800CL	Ocean surface processes, wave kinematics and breaking, frontal processes
Hyperspectral Camera	Specim EagleAISA	Ocean surface and biogeochemical processes
GPS/IMU Novatel SPAN-LN200		Georeferencing, trajectory

Sea surface topography collected from MASS lidar
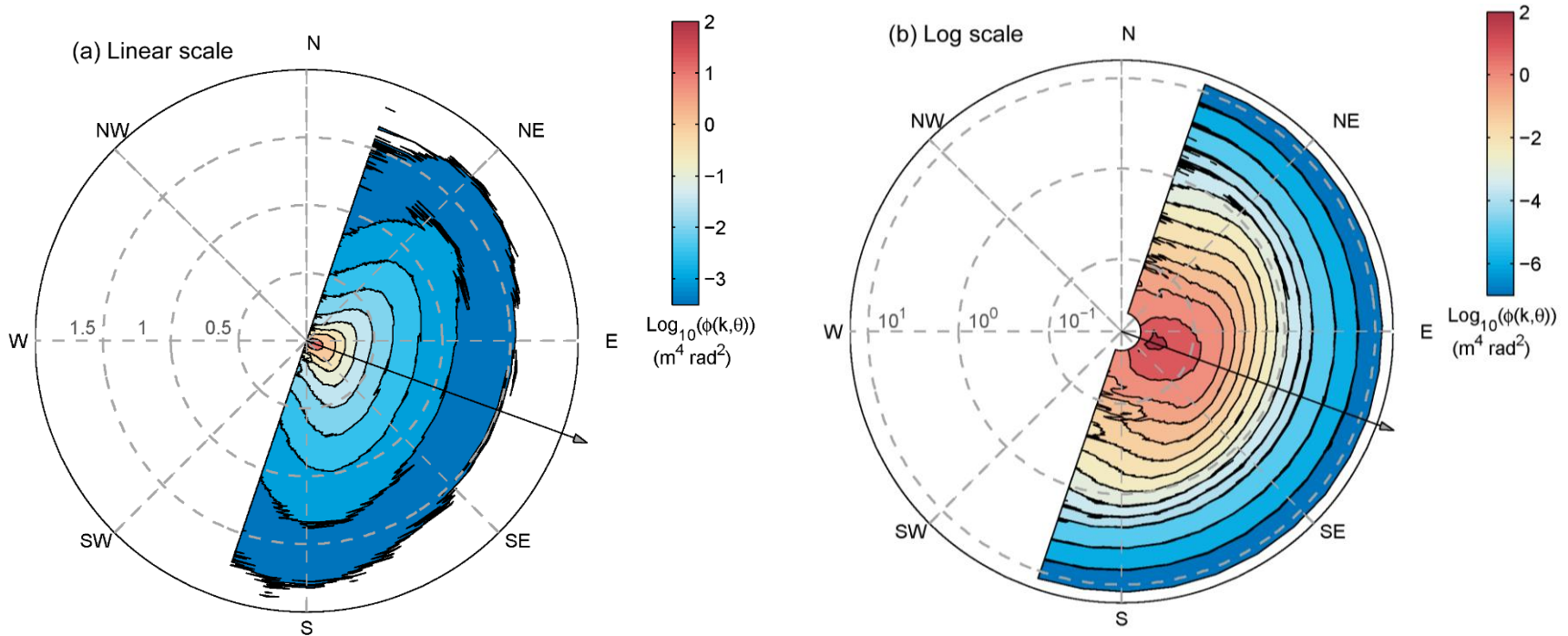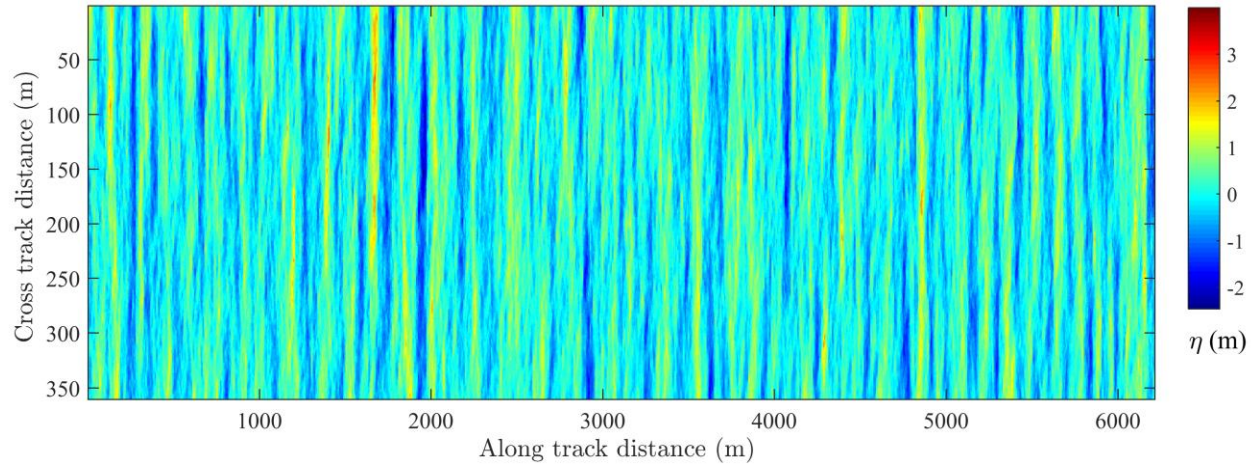
Bimodality of directional wave spectrum found in earlier work for smaller wavenumbers (Hwang et al. 2000a,b; Romero and Melville 2010a, Leckler et al. 2015, Peureux et al. 2018)
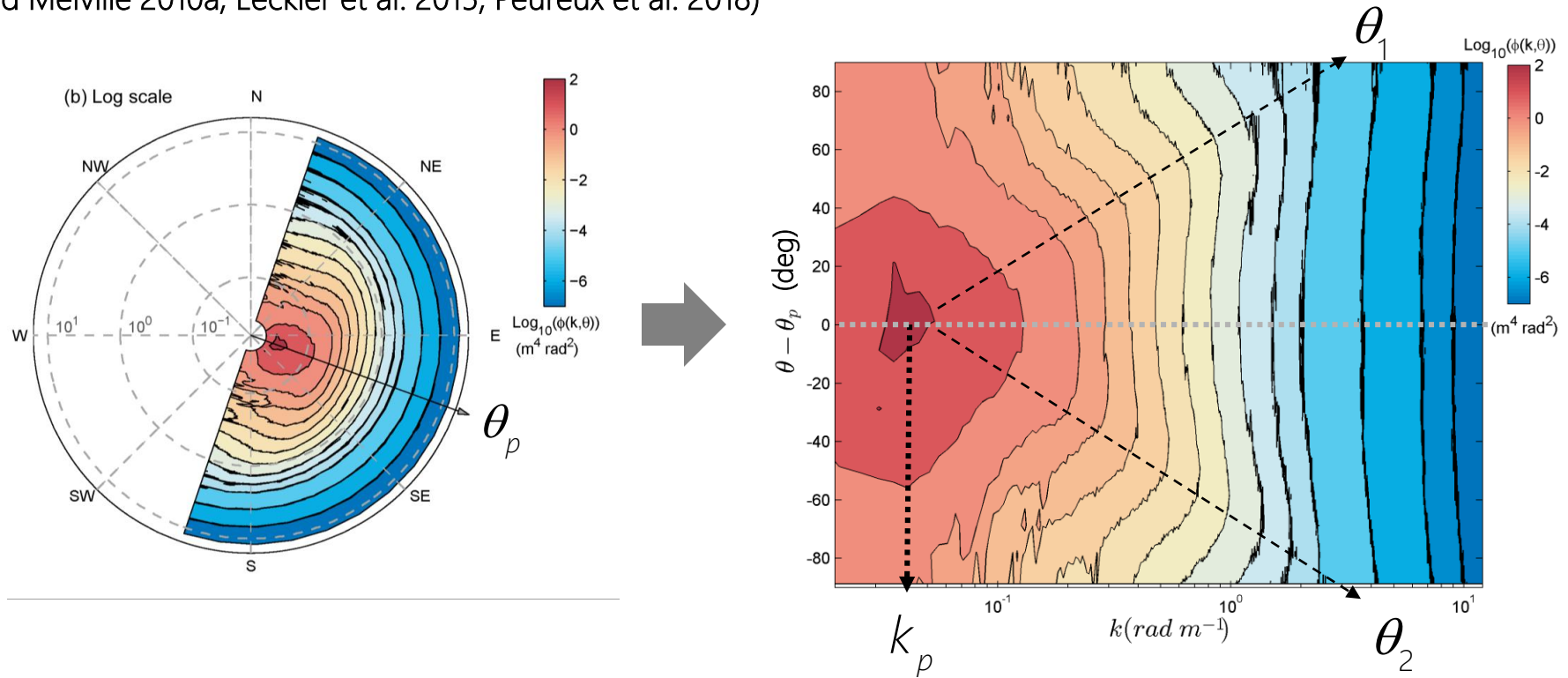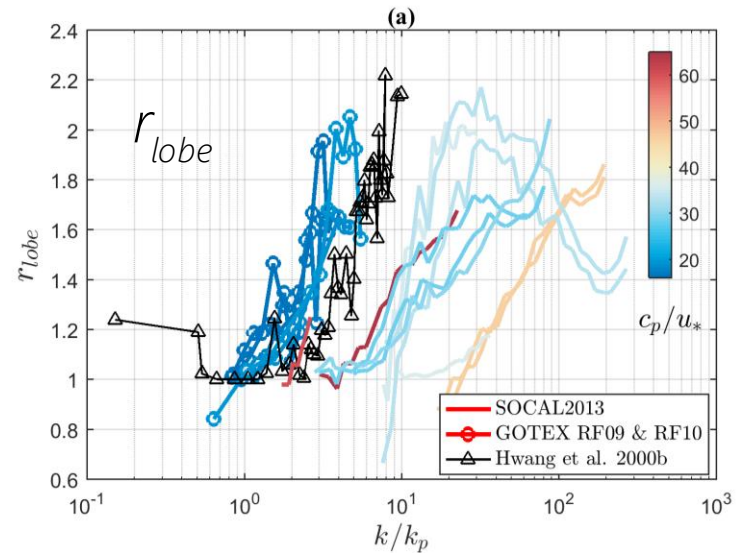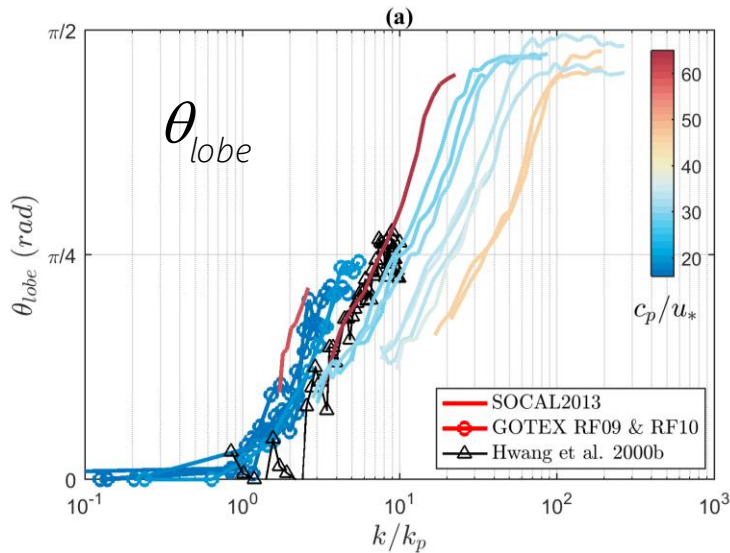

Azimuthal lobe separation
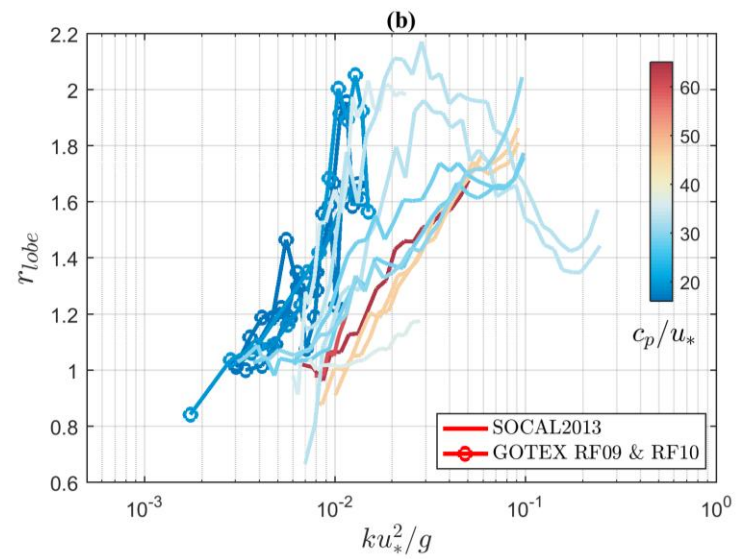
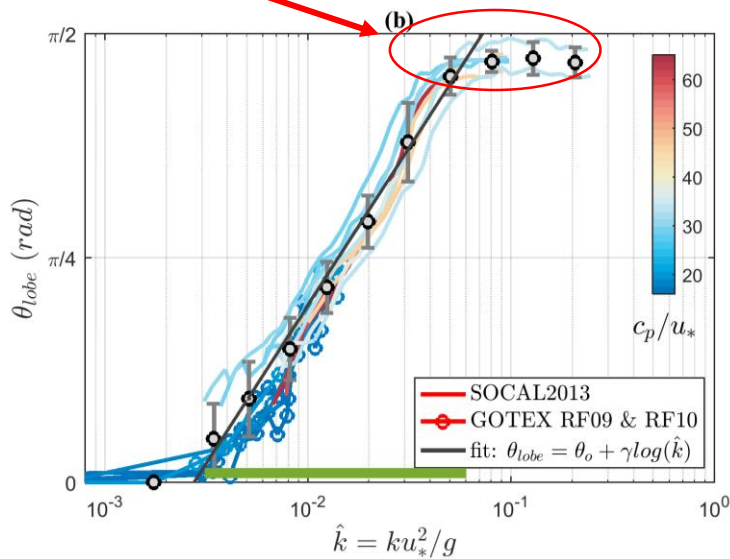$$\theta_{lobe} = \frac{|\theta_1 - \theta_2|}{2}$$

Average lobe amplitude relative to the spectral energy in the dominant wave direction

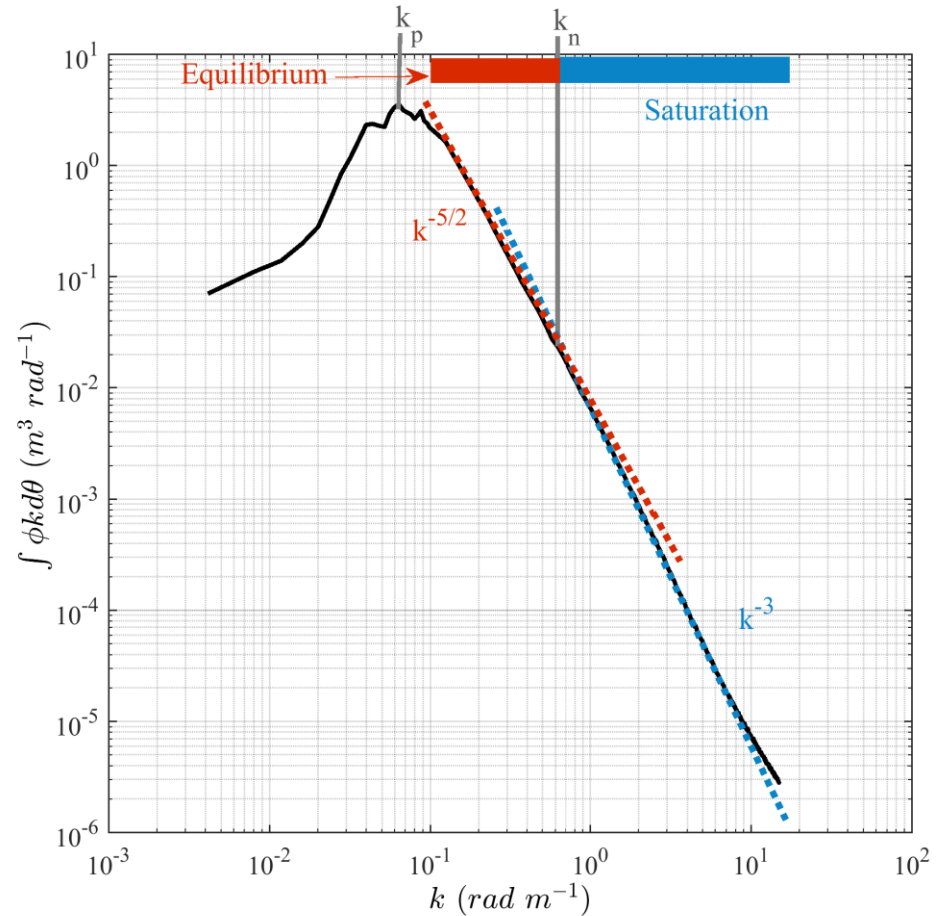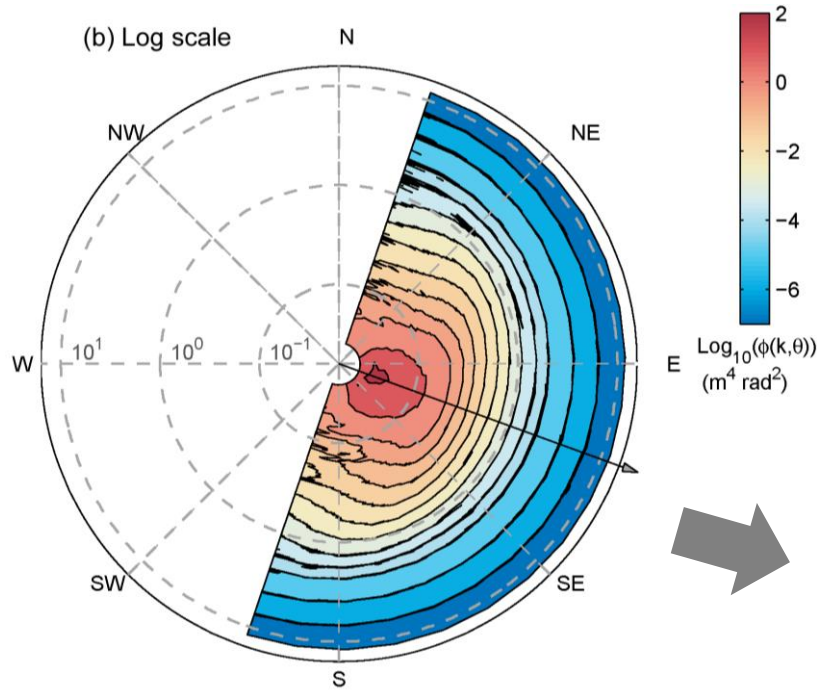$$r_{lobe} = \frac{|\phi(k,\theta_1) + \phi(k,\theta_2)|}{2\phi(k,0)}$$

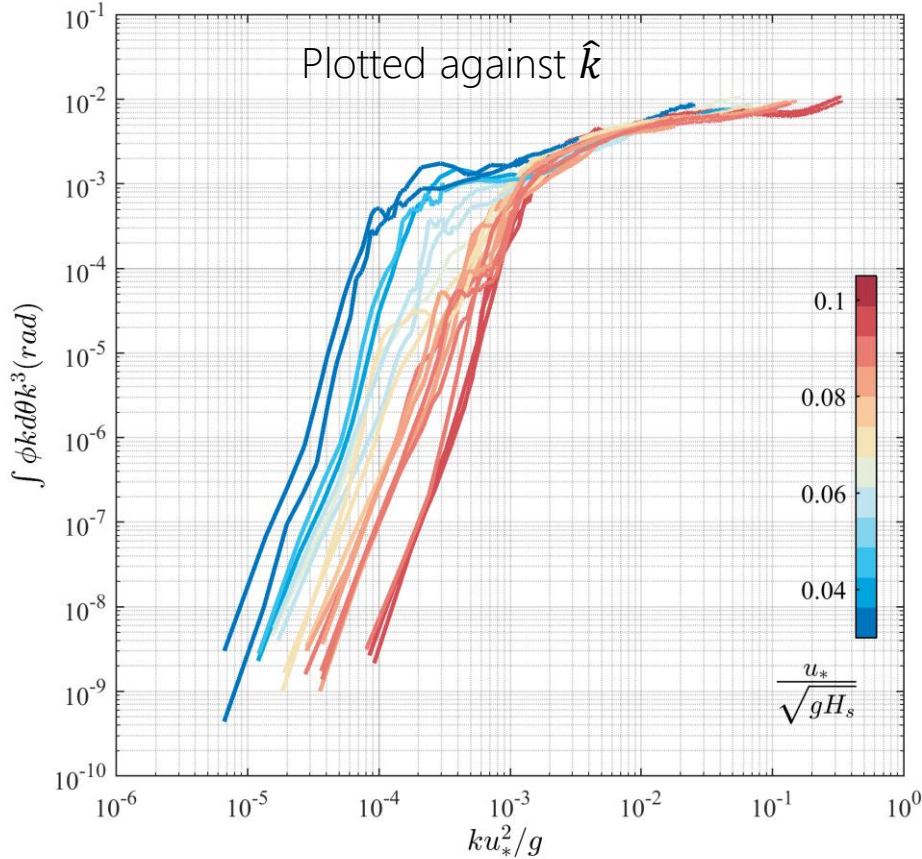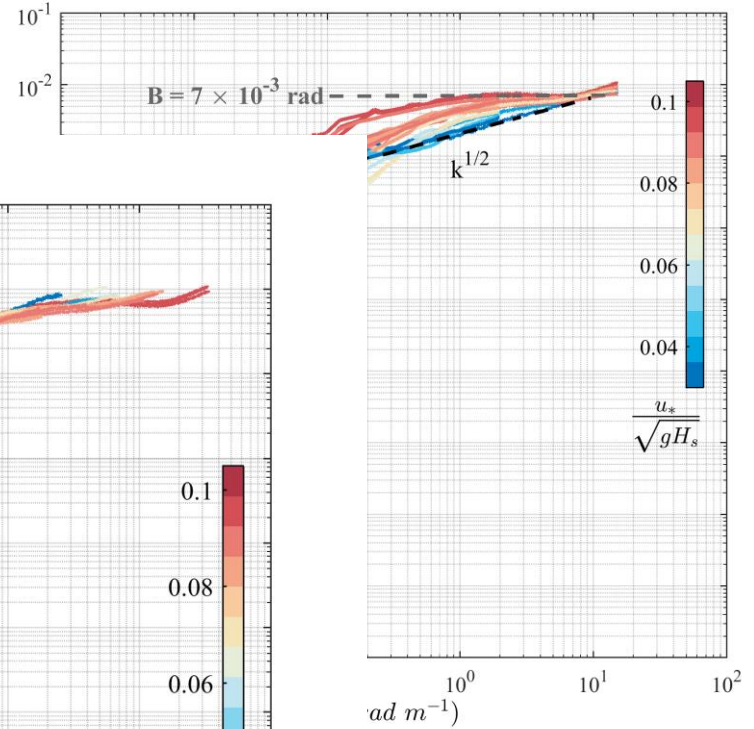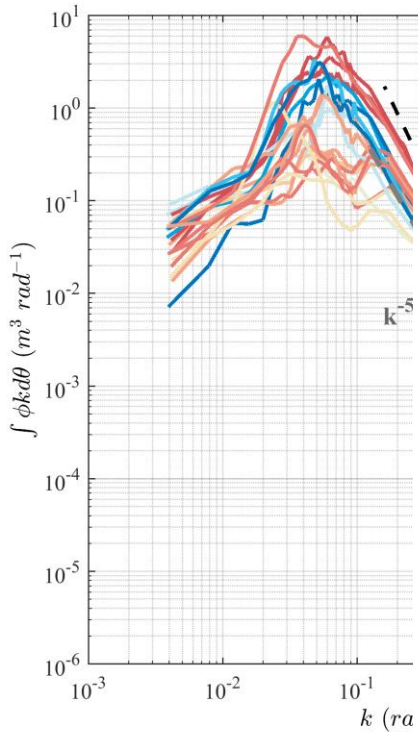Non-dimensional $\hat{k}$ based on Phillips 1985 scaling of the upper limit of the equilibrium spectrum

Consistent with Phillips 1985 equilibrium model and our understanding of the saturation range

SCRIPPS INSTITUTION OF
OCEANOGRAPHY *UC San Diego*

Plotted against $\hat{k}$

$B = 7 \times 10^{-3}$ rad

$k^{1/2}$

k^{-5}

All spectra collected duri[...] a broad range of envi[...]

[...]turation spectra

SCRIPPS INSTITUTION OF
OCEANOGRAPHY UC San Diego
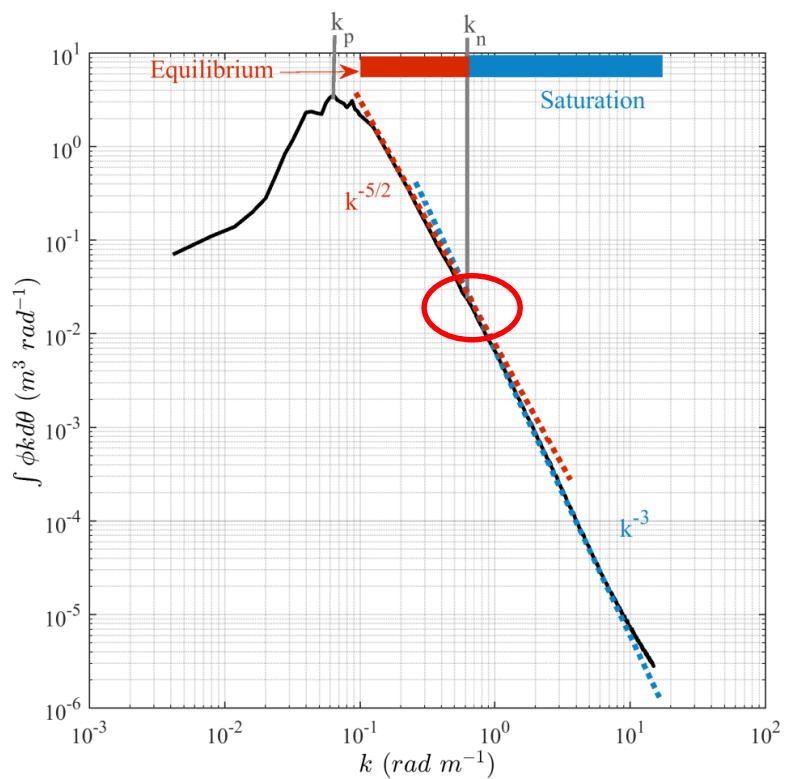
Lenain, Pizzo & Melville, manuscript in preparation
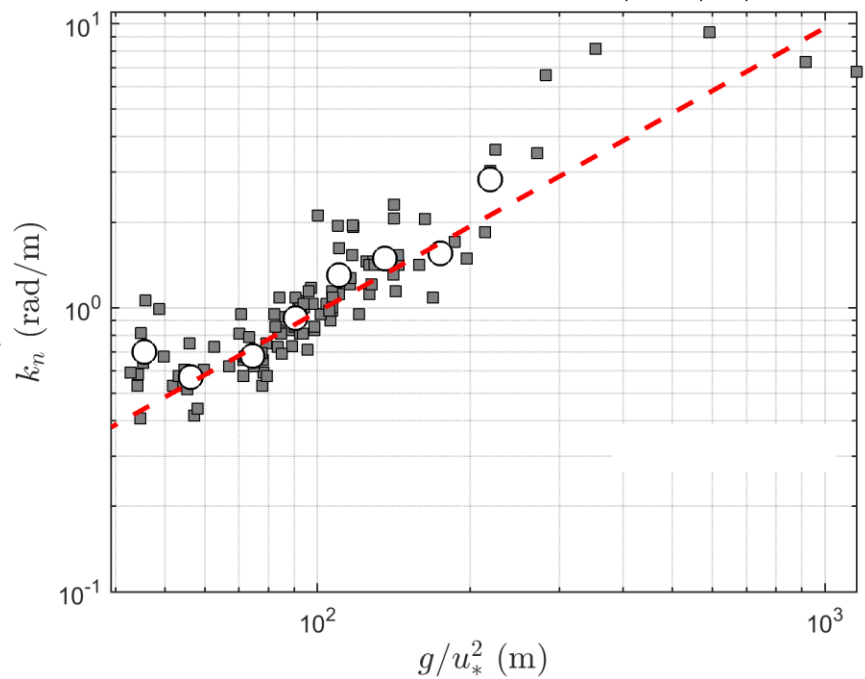
Using SOCAL2013,LCDRI2017 & ISDRI2017 experiments

Fitting equilibrium and saturation ranges to determine intersect point located at k_n

Consistent with Phillips (1985)

Crucial for wind-wave modelling and upper ocean studies (i.e. Stokes drift requires accurate depiction of the spectral shape across the equilibrium-saturation ranges)

Stokes drift ➡ Langmuir turbulence number

Equilibrium range contributes to only 10-30% of mean square slope

Fraction

(note that wave buoys generally only resolve the equilibrium range)
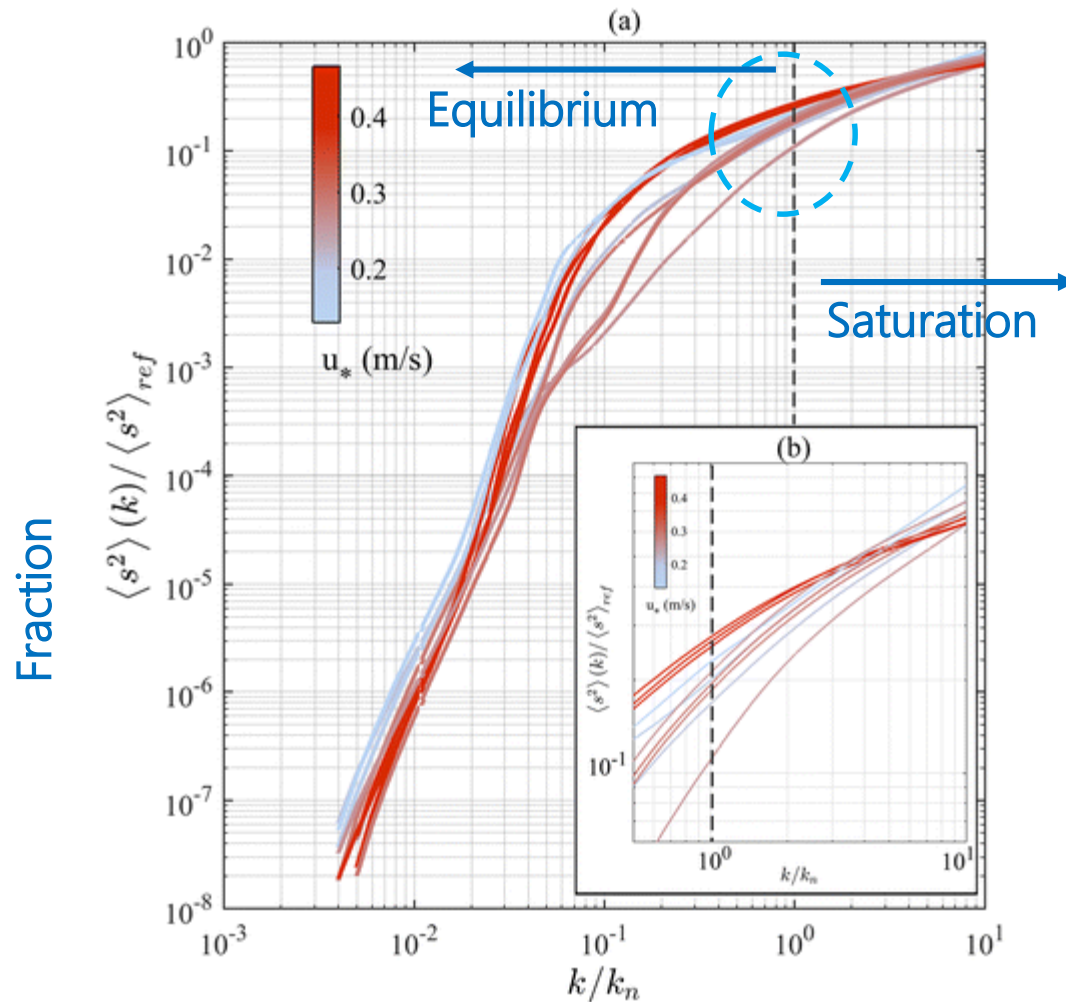

(a) Total spectral mean square slope $\langle s^2 \rangle$ (k) computed from the omnidirectional wave spectrum, normalized by the total mean square slope defined by Cox and Munk (1954), $\langle s^2 \rangle_{ref}$ and plotted against the normalized wavenumber k/k_n. (b) A zoomed-in version of the same plot, focusing on the higher-wavenumber portion. The normalized wavenumber reference band $k/k_n = 1$ is shown as a black dashed line.

SCRIPPS INSTITUTION OF **OCEANOGRAPHY** *UC San Diego*

estimating surface slope statistics and wind speed and momentum flux <u>remotely</u>
Novel lidar based technique, following the seminal work of Cox & Munk 1956.
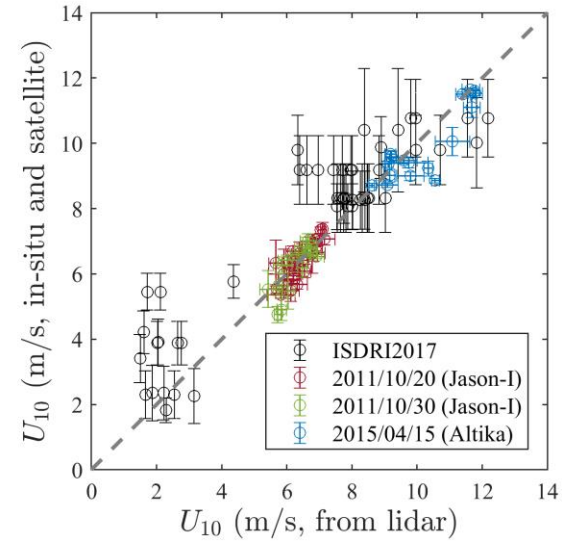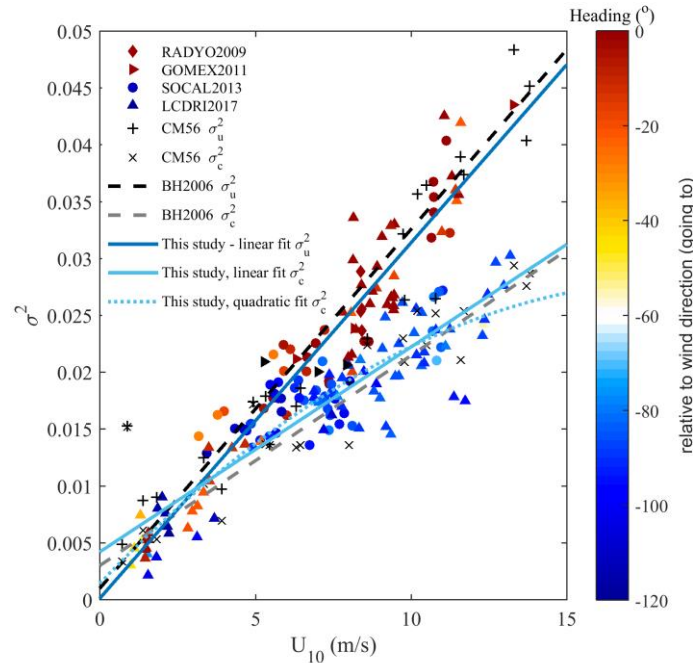
Significant spatio-temporal variability in atmospheric forcing across op. area while limited in-situ sampling from ships, buoys and swift platforms

Wind speed   4hr flight
(derived from MASS airborne lidar)

Manuscript to submitted JPO, under review (Lenain, Statom & Melville)
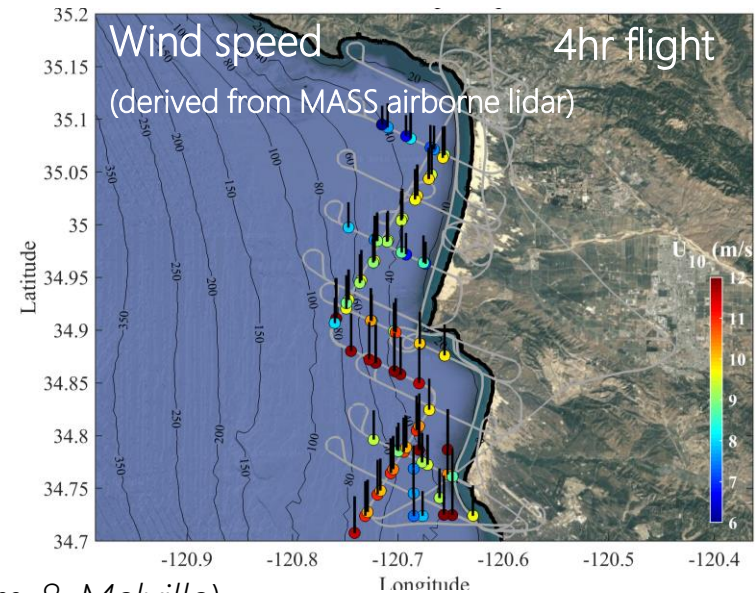
- Unique data set of directional measurements of surface waves ranging from kilometers to sub-meter scales, collected from a novel airborne lidar system characterizing the directional properties of the wave field across the equilibrium-saturation ranges over broad range of environmental conditions.

- Measurements extend the known bimodal distribution well beyond what was previously reported, showing for the first time that waves of opposing direction, orthogonal to the wind direction, can be generated in a single storm system (implications for acoustics, wave modelling etc...)

- Omnidirectional spectra show power law consistent with the equilibrium model of Phillips (1985) and the saturation range power law found in other recent studies. We also found a remarkable agreement and collapse of the spectra using u_*^2/g, to non-dimensionalize the wavenumber.

- A new parameterization of the upper wavenumber limit of the equilibrium range is proposed.

- Lidar derived slope statistics showing good agreement with the seminal results of Cox & Munk (1954) for the mean-square slope and more recent work based on satellite remote sensing (Breon & Henriot 2006), but with significant discrepancies for the higher order statistics (not shown here).